lubricants

MDPI

Article

Investigation of Anti-Friction Properties of MoS_2 and SiO_2 Nanolubricants Based on the Friction Pairs of Inconel 718 Superalloy and YG6 Carbide

Lijie Ma [1,*], Fengnan Li [1], Shijie Ba [1], Zunyan Ma [2], Xinhui Mao [2], Qigao Feng [1,*] and Kang Yang [3]

[1] School of Mechanical and Electrical Engineering, Henan Institute of Science and Technology, Xinxiang 453003, China
[2] School of Mechanical and Power Engineering, Harbin University of Science and Technology, Harbin 150080, China
[3] Department of Mechanical Engineering, Anyang Institute of Technology, Anyang 455000, China
* Correspondence: ma_lj@hist.edu.cn (L.M.); fqg@hist.edu.cn (Q.F.); Tel.: +86-0373-304-0394 (L.M.); +86-0373-304-0394 (Q.F.)

Abstract: In order to improve the anti-friction property of common mineral oil and develop a high-performance lubricant, MoS_2 and SiO_2 nano-additives were individually dispersed into the 350SN mineral oil at various weight percentages to prepare nanolubricants. Then, the viscosity, wettability, and tribological properties of the nanolubricants were measured and analyzed with a rotary viscometer, a contact angle measuring instrument, and a friction tester. Finally, the action mechanism of two nano-additives was explained based on the energy spectrum test results of the abrasion surface. The results show that MoS_2 and SiO_2 nano-additives could improve the viscosity of the base fluid and change its wettability, giving nanolubricants better anti-friction performance than the base fluid. Due to the difference in physical properties, SiO_2 and MoS_2 nanolubricants presented different friction reduction rules with the increase in nano-additive percentage. Under experimental conditions, SiO_2 nanolubricants showed better anti-friction effects than MoS_2 nanolubricants. When the SiO_2 percentage was 10 wt% and 15 wt%, the maximum friction coefficient was reduced to 0.06, which was about 1/3 of that with the base fluid. In this case, the abrasion surface quality was significantly improved, and the abrasion trace size was about half that of the base fluid. The energy spectrum test results show that the action mechanism of the MoS_2 nano-additive is the adsorption film effect and mending effect of nanoparticles, while the main action mechanism of the SiO_2 nano-additive should be the polishing effect and rolling effect of nanoparticles.

Keywords: anti-friction properties; nanolubricant; MoS_2; SiO_2; friction coefficient; abrasion surface topography; abrasion trace size; mechanism

check for updates

Received: 9 November 2024
Revised: 15 December 2024
Accepted: 25 December 2024
Published: 27 December 2024

Citation: Ma, L.; Li, F.; Ba, S.; Ma, Z.; Mao, X.; Feng, Q.; Yang, K. Investigation of Anti-Friction Properties of MoS_2 and SiO_2 Nanolubricants Based on the Friction Pairs of Inconel 718 Superalloy and YG6 Carbide. *Lubricants* **2025**, *13*, 4. https://doi.org/10.3390/lubricants13010004

Copyright: © 2024 by the authors. Licensee MDPI, Basel, Switzerland. This article is an open access article distributed under the terms and conditions of the Creative Commons Attribution (CC BY) license (https://creativecommons.org/licenses/by/4.0/).

1. Introduction

Friction is a common phenomenon in the process of mechanical operation and is also the main cause of energy loss and mechanical failure [1]. Lubrication is the main way to reduce energy waste and restrain mechanical wear. According to the different mediums, lubrication methods can be divided into fluid lubrication, solid lubrication, and semi-solid lubrication, of which fluid lubrication is the most widely used one [2]. Nanofluid lubrication is an emerging efficient fluid lubrication technology that has become one of the research highlights in the field of tribology [3–5].

During nanofluid lubrication, nanoscale particle additives are dispersed into the base liquid (including water, emulsion, oil, etc.) to prepare nanolubricants, which improves the lubrication effect of the base liquid through the adhesion, filling, embedding, and rolling of nano-additives between the friction interfaces [6,7]. At present, many nanoparticles can be used to prepare nanolubricants, including metals, metal oxides, sulfides, nanocomposites, and carbon nanotubes; most of them have a large specific surface area, a high chemical activity, and excellent friction reduction characteristics [8,9]. Therefore, nanolubricants have many advantages over common lubricants, such as high thermostability, high load capacity, high efficiency, and low pollution.

Due to the differences in physicochemical properties of nano-additives, nanolubricants with various additives have different anti-friction performance and mechanism. Jatti et al. [10] found that the CuO nano-additive could be brought into the moving friction pairs of LM6 aluminum alloy and EN31 bearing steel to transform sliding friction into rolling friction, thereby reducing the shear resistance and improving the lubricating performance of machine oil. Sia et al. [11] disclosed that the SiO_2 nano-additive could roll into the friction interface of chrome-plated carbon steel bearings to fill and repair the defective area, decreasing the friction temperature and wear rate. Sujan et al. [12] studied the influence of mixed Al_2O_3 and WS_2 additives on the anti-friction performance of the base fluid. Their results show that the Al_2O_3 nanoparticles with a higher hardness could be pressed into the friction surface, reducing the wear rate, while the flaky WS_2 microparticles were adsorbed on the friction surface to form a solid lubricating film, thereby decreasing the friction coefficient. Su et al. [13] investigated the performance of graphite nanolubricants with LB2000 vegetable oil as the base fluid and found that graphite additives form a physical deposition film between friction interfaces, thereby decreasing the friction coefficient and the wear rate, and the nano-additives with a 35 nm size exhibited better anti-friction performance than the nano-additives with an 80 nm particle size. The research by Yu also showed that MoS_2 nanoparticles could form an isolation layer between friction interfaces, thus preventing the direct contact of frictional pairs and reducing the fluctuation and amplitude of the instantaneous friction coefficient [14].

In addition to the properties of nano-additives, the additive percentage is also an important factor in the performance of nanolubricants. Mo et al. [15] developed several Sn nanolubricants with different additive percentages and applied them to the wear resistance tests between steel–brass friction pairs, with the results showing that Sn nanolubricants could repair the worn surface, and the higher the additive percentage is, the better the repair effect. Singh et al. [16] carried out lubricating performance tests of SiO_2 nanolubricants through pin-on-disc frictional experiments. Their results show that the friction coefficient and the wear rate first decreased and then increased with the rise in the SiO_2 percentage, and the lowest friction coefficient and the best abrasion trace morphology were achieved when the SiO_2 percentage was 0.6 wt%. However, when the SiO_2 percentage exceeded 1.2 wt%, the SiO_2 nanolubricant could not perform better than the base oil. Chu et al. [17] studied the anti-friction performance of diamond nanolubricants using ring-on-block friction tests on SKD11 and SKD61 steel and found that when the additive percentage was 2 vol%, the friction coefficient was the minimum, and when the additive percentage was 3 vol%, the wear rate was the lowest. Gupta et al. [18] investigated the property of graphite nanolubricants through four-ball frictional experiments, and the results indicate that the wear scar size also exhibited a changing trend of decreasing first and then increasing with the rise in the additive percentage, and the wear rate was the lowest when the additive percentage was 3 wt%. The research of Luo disclosed that when Al_2O_3 nanolubricants were applied in the four-ball and thrust-ring friction tests, the Al_2O_3 nanoparticles adhered to the friction surface to form a self-laminating protective film, and the 0.1 wt% nanolubri-

cant displayed a better anti-friction performance than the 0.05 wt%, 0.5 wt%, and 1 wt% nanolubricants [19].

In recent years, the application of nanolubricants in the field of transportation, electronics equipment, nuclear systems, and machining operations has also achieved some good results. Peyghambarzadeh et al. [20] found that Al_2O_3/water nanolubricant can enhance heat transfer efficiency by 45% in the automobile radiator than pure water. The research of Mohamed [21] also showed that the nanolubricant dispersed with copper (Cu) and graphene (Gr) nanoparticles in a fully formulated engine oil is a promising lubricating medium for increasing the durability of frictional sliding components and fuel economy in automobile engines. Kulkarni et al. [22] applied Al_2O_3 nanolubricant as a coolant in a diesel–electric generator to reduce equipment temperature. Buongiorno [23] discovered that nanolubricants have potential applications in improving the economy and safety of nuclear reactors. Syafiq et al. [24] carried out a minimum quantity lubrication (MQL) research with SiO_2 nanolubricant during the turning of Al319 aluminum alloy and found that the cutting temperature decreased and the surface roughness improved compared with the common MQL lubricant, and the best effect was achieved at the 0.5 wt–1.5 wt% SiO_2 percentage. Ni et al. [25] conducted the broaching tests on AISI 1045 steel under the CuO nanolubricant and found that the maximum broaching force was decreased to 62.7% of that of pure sesame oil when the CuO percentage was approximately 0.54 wt%. According to the drilling test on AISI321 stainless steel, Pal et al. reported that the Al_2O_3 nanolubricant could significantly improve the machining quality and the tool life compared with the common MQL lubricant [26].

In summary, nano-additives can significantly improve the anti-friction properties of the base fluid, and the type and percentage of nano-additives are two important parameters that affect the anti-friction properties of nanolubricants. Nowadays, although some progress has been made in the application of nanolubricants in the machining field, most of the related research is still focused on easy-to-machining materials, such as aluminum alloy, copper alloy, and medium carbon steel.

As a kind of common industrial raw material, mineral oil is widely applied as a lubricant and coolant in the field of machining. However, with the industrial application of a large number of difficult-to-machining materials, common mineral oil has been difficult to meet the practical needs of this field [27,28]. In this study, eight nanolubricants were prepared by dispersing different weight percentages of MoS_2 and SiO_2 additives into 350SN mineral oil. Then, the viscosity, wettability, and tribological properties of the nanolubricants were intensively investigated. Finally, the anti-friction mechanisms of the two nano-additives were discussed. This study helps reveal the action mechanism of nano-additives, enriches the theory of particle tribology, and has an important practical value to the development and application of high-performance lubricants.

2. Material and Methodology

2.1. Preparation of Nanolubricants

To compare the anti-friction effect of different nano-additives, MoS_2 and SiO_2 particles with large property differences were selected as additives. MoS_2 is a common soft lubricating material with a small friction coefficient (0.04–0.09) and good chemical and thermal stability. It is widely applied in the aerospace, casting, and forging industries. SiO_2 is a typical hard and brittle material with excellent high-temperature performance and chemical stability and is widely used as an antiadhesion agent or flow aid in the industrial field [29–31]. The particle size of the two additives is approximately 30 nm, and their morphology and physical properties are shown in Figure 1 and Table 1, respectively. In this study, 350SN mineral oil produced by Jinan Xinhuihuang Chemical Co., Ltd. was

selected as the base fluid. It is a commonly used industrial oil that can not only be used independently as a lubricant in the manufacturing field but also as a base liquid. The main properties of 350SN mineral oil are listed in Table 2.

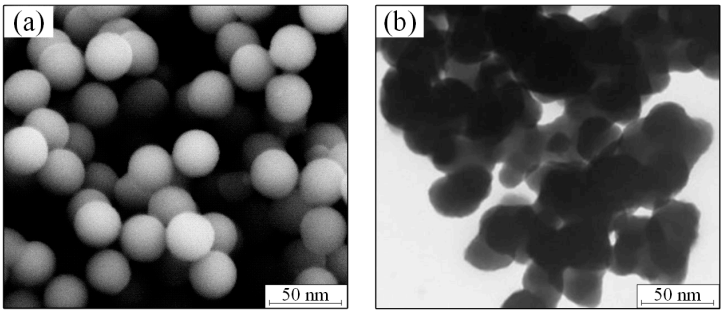


Figure 1. SEM images of nano-additives: (**a**) SiO_2 (**b**) MoS_2.

Table 1. Physical properties of SiO_2 and MoS_2 nano-additives.

Nanoparticle	Molecular Weight	Density (g/cm^3)	Melting Point (°C)	Moh's Hardness
SiO_2	60.08	2.2–2.6	1723	7
MoS_2	160.07	4.8	2375	1.0–1.5

Table 2. Properties of 350SN mineral oil.

Indexes	Density	Kinematic Viscosity (40 °C) (mm^2/s)	Flash Point (°C)	Pour Point (°C)
Value	0.87	62–68	238	−12

The nano-additives have large surface energy and specific surface area, which makes them easy to agglomerate in the base fluid [32,33]. To improve their dispersibility, according to references [34,35], KH-550 (γ-Aminopropyl triethoxysilane) and SP80 (Sorbitol fatty acid ester) were applied as the dispersants of SiO_2 and MoS_2 nano-additives, respectively, which have good dispersion effect on nano-additives and have little impact on the properties of the base fluid. The dosage of the dispersants was approximately 50% of the weight of nano-additives [34,35]. In light of our pre-machining tests on nickel-based alloy, it was difficult for the nanolubricant with a low additive percentage to have a better anti-friction effect than the base fluid. Therefore, the weight percentage of the nano-additive was determined to be 5 wt%, 10 wt%, 15 wt%, and 20 wt%. On the basis of the above, different proportions of base fluid, nano-additive, and dispersant were mixed together. Then, the mixture was stirred with a magnetic stirrer and oscillated with an ultrasonic oscillator for 30 min to obtain the nanolubricants. Figure 2 shows the eight nanolubricants prepared in this research.

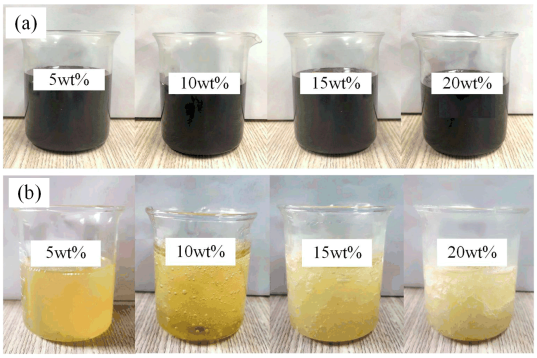


Figure 2. Nanolubricants: (**a**) MoS_2; (**b**) SiO_2.

2.2. Viscosity and Wettability Test of Nanolubricants

Viscosity is an important indicator for evaluating the fluidity of nanolubricants, which is closely related to the lubricating and cooling performance [36,37]. As shown in Figure 3a, a NDJ-5s rotary viscometer (Wincom, Changsha, China) was used to measure the dynamic viscosity. Given that MoS_2 nanolubricants are similar to Newtonian fluids, their viscosities were measured using the traditional Newtonian fluid viscosity measurement method. SiO_2 nanolubricants have obvious shear thinning and thixotropic features, and their viscosities decrease gradually with the increase in shear time [38,39]. Therefore, the viscosity values at the 120 s shear time were recorded as the final result.

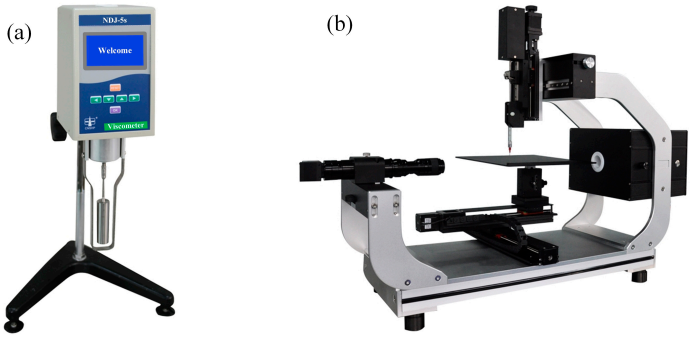


Figure 3. Viscosity and wettability test equipment: (**a**) NDJ-5s rotary viscometer; (**b**) SDC-100 contact angle measuring instrument.

The wettability was evaluated by the contact angle of the droplet spreading, which was tested using a SDC-100 contact angle measuring instrument (SINDIN, Dongguan, China) (see Figure 3b). In this measurement, a 15 mm × 15 mm × 3 mm Inconel 718 superalloy rectangular block with surface roughness Ra 150 nm was used for droplet spreading, and the same sample was also used as the lower specimen for the subsequent friction test. Before the measurement, the samples were ultrasonically cleaned in a 5 vol% acetone aqueous solution for 20 min and then wiped with ethanol absolute and dried at room temperature. For each lubricant, the mean of five tests was taken as the final result.

2.3. Tribological Tests and Conditions

As shown in Figure 4, the friction test was carried out on a MWF-500 ball-on-disk reciprocating friction tester (MWF Detector, Singapore). The lower specimen was an Inconel 718 rectangular block, and its chemical composition and mechanical properties are shown in Tables 3 and 4, respectively. Inconel 718 superalloy has excellent physical mechanics properties such as high strength, good toughness, high-temperature resistance, and corrosion resistance, and it is widely used in the field of aviation, aerospace, and nuclear industries. However, it is also a typical difficult-to-cutting material that requires

high-performance cutting lubricants [40]. The upper specimen was a YG6 cemented carbide ball with a diameter of ϕ6.5 mm and a surface roughness of Ra 25.4 nm. YG6 is a common tool material, and its chemical composition and mechanical properties are shown in Table 5. In this research, the anti-friction properties of lubricants are evaluated by friction coefficient, surface topography, and abrasion trace size of the lower specimen. In order to reduce the experimental error, a new YG6 upper specimen was used for each friction test.

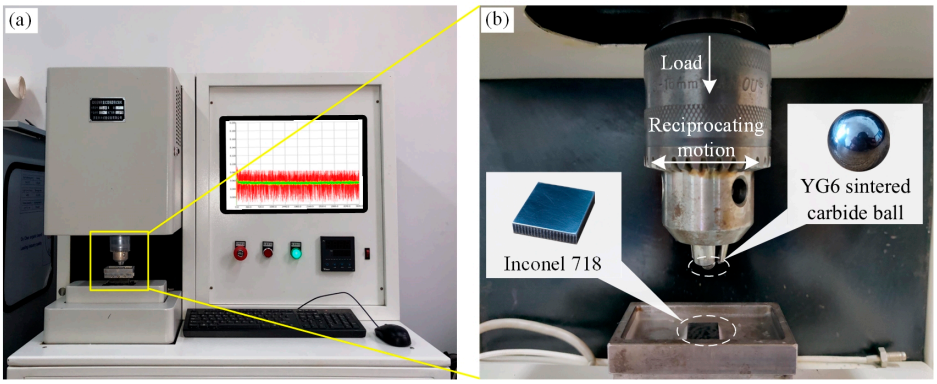


Figure 4. Friction tester and the specimens: (**a**) MWF-500 friction tester; (**b**) lower and upper specimens.

Table 3. Chemical composition of Inconel 718 superalloy.

Chemical Element	Ni	Cr	Nb	Mo	Ti	Al	Co	C	Mn	Si	P	S	B	Cu	Fe
Minimum value	50.0	17.0	4.75	2.8	0.65	0.2	—	—	—	—	—	—	—	—	Margin
Maximum value	55.0	21.0	5.50	3.3	1.15	0.8	1.0	0.08	0.35	0.35	0.015	0.015	0.006	0.3	

Table 4. Mechanical properties of Inconel 718 superalloy.

Yield Strength MPa	Tensile Strength MPa	Elongation %	Poisson Ratio GPa	Thermal Conductivity W/m·K	Density g/cm^3	Hardness HV
1110	1310	23.3	206	11.2	8.47	281

Table 5. Chemical composition and mechanical properties of YG6 cemented carbide.

Co Content %	WC Content %	Flexure Strength MPa	Impact Toughness J/cm	Poisson Ratio GPa	Hardness HRA	Density g/cm^3
6	94	145	2.6	530	89.5	14.6–15.0

To improve the accuracy of friction test, the friction surface of the Inconel 718 specimen was pre-polished to a roughness of approximately Ra 150 nm. The surface topography of the specimen was shown in Figure 5, where different colors indicate surface fluctuation. During the test, the Inconel 718 specimen was bonded on the bottom of the cargo tank using paraffin wax, the upper specimen was fixed by an elastic chuck, and the friction pairs were lubricated by the lubricants in the cargo tank. Other test conditions include the following: the friction time was 60 min, the distance and frequency of reciprocating motion was 4 mm and 2.5 Hz, the normal load was 80 N, and the testing temperature was room temperature (approximately 20 °C).

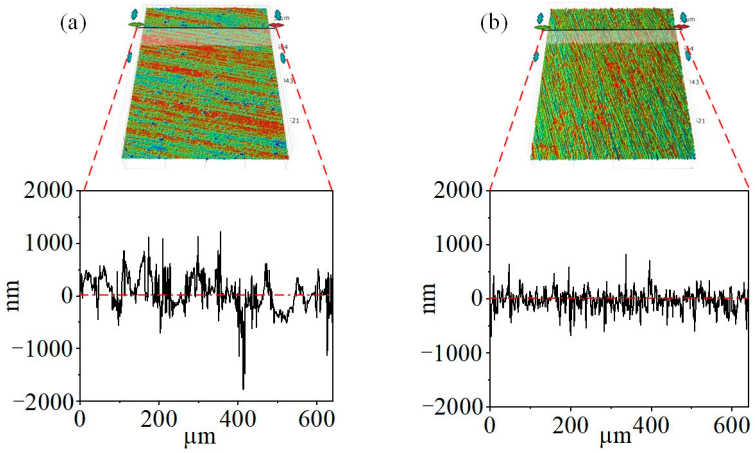


Figure 5. Friction surface of Inconel 718 specimen before and after polishing: (**a**) before polishing; (**b**) after polishing.

3. Results and Discussion

3.1. Viscosity and Wettability of Nanolubricants

3.1.1. Viscosity

The room temperature dynamic viscosities of the nanolubricants are shown in Figure 6. According to Figure 6, for both MoS_2 and SiO_2 nanolubricants, the viscosities increased significantly with the additive percentage. However, due to the prominent thickening effect of the SiO_2 nano-additive, the viscosities of the SiO_2 nanolubricants were much higher than those of the MoS_2 nanolubricants. Although 20 wt% SiO_2 nanolubricants still have certain flowability and can be used for lubrication in low-speed machining processes, their viscosity can no longer be measured using a NDJ-5s rotary viscometer.

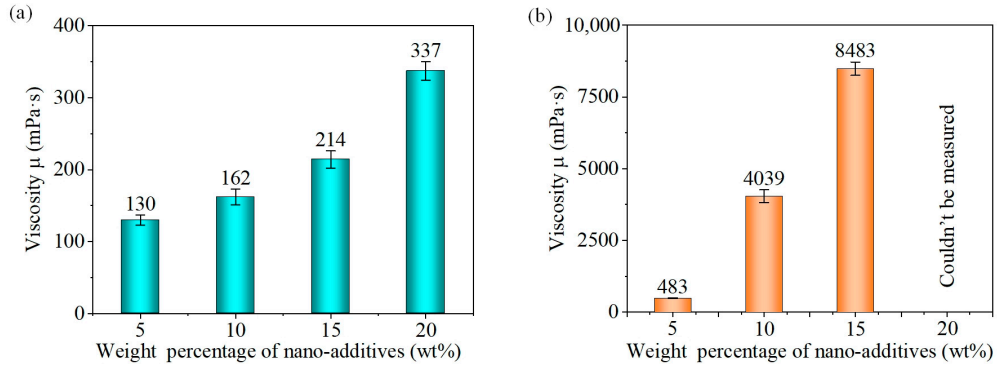


Figure 6. Viscosities of nanolubricants. (**a**) MoS_2; (**b**) SiO_2.

3.1.2. Wettability

Figure 7 shows the contact angles of the base fluid and the nanolubricants, and a small contact angle means that the lubricant has good wettability. The following results can be obtained from Figure 7.

(1) The contact angles of the MoS_2 nanolubricants were smaller than that of the base fluid and decreased gradually with the increase in the additive percentage. This phenomenon indicates that the MoS_2 nanolubricants can easily form an adsorption film on the surface of the Inconel 718 superalloy. Moreover, the higher the additive percentage within the test range is, the better the wettability is.

(2) With the increase in the additive percentage, the contact angles of the SiO_2 nanolubricants presented a completely different variation rule. The contact angle of the 5

wt% SiO_2 nanolubricant is smaller than that of the base fluid, while that of the 10 wt% SiO_2 nanolubricant was 67.81°, which is much larger than that of the base fluid. With the further increase in the additive percentage, the droplets displayed an irregular shape on the sample surface due to poor fluidity, making it impossible to measure the contact angle. This phenomenon shows that the SiO_2 nanolubricants cannot easily form an adsorption film on the surface of the lower specimen, and their wettability becomes bad and can even be lost as the additive percentage increases.

The above results indicate a certain correlation between the viscosity and wettability of nanolubricants. However, due to the differences in physical properties of nano-additives, the wettability of MoS_2 and SiO_2 nanolubricants exhibited different variation features with their viscosity. With the increase in the additive percentage, the wettability of the MoS_2 nanolubricants increased with the viscosity, while the wettability of the SiO_2 nanolubricants decreased.

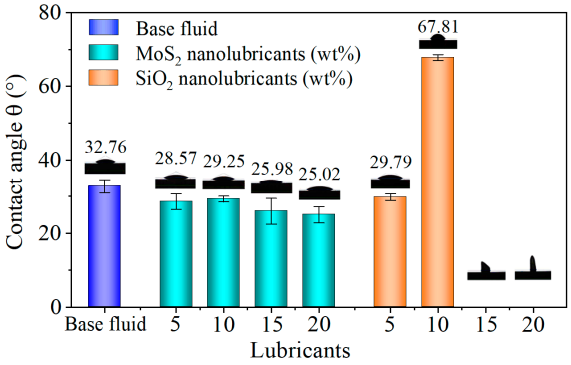


Figure 7. Contact angles of base fluid and nanolubricants.

3.2. Anti-Friction Properties of Different Lubricants

3.2.1. Friction Coefficient

Base Fluid

Figure 8 shows the friction coefficient curve under the lubrication of the base fluid and the abrasion surface morphologies of the Inconel 718 specimen. The repeated tests indicated that the friction coefficient presented a three-stage change trend with the friction time, and the characteristics of the three stages are "low amplitude stable fluctuation", "high amplitude slow decrease", and "low amplitude stable fluctuation", respectively. In order to clarify the reason for the change in friction coefficient, the surface morphologies of the lower specimen were acquired in the middle of each stage. According to Figure 8, there is a close relationship between friction coefficient and abrasion surface morphologies.

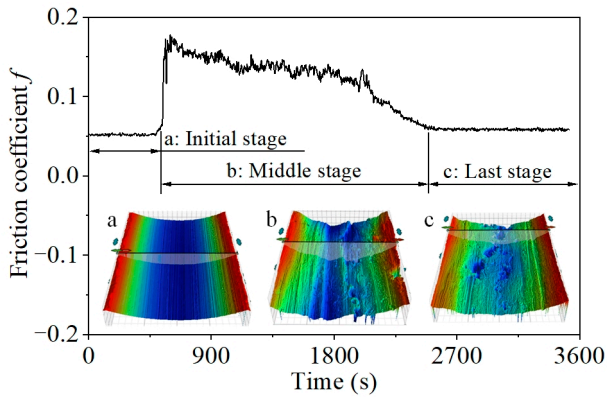


Figure 8. Friction coefficient curve under the lubrication of the base fluid.

(1) In the initial stage, the mean friction coefficient was lowest, approximately 0.052, and the abrasion surface was relatively smooth. In this case, the friction type should be boundary friction, and a stable lubricating film should exist at the friction interface.
(2) In the middle stage, the instantaneous friction coefficient increased sharply and reached 0.178, then showed a slow downward trend. At the same time, some furrows appeared on the abrasion surface. It can be inferred that serious adhesive and abrasive wear happened on the surface of the Inconel 718 specimen, and the friction type should be mixed friction where dry friction and boundary friction coexist. However, the appearance of furrows reduced the contact area of two specimens and increased the unit contact pressure. As a result, the furrows were gradually smoothed out with the rise of friction time, resulting in a gradual decrease in the instantaneous friction coefficient.
(3) In the last stage, the abrasion surface quality was significantly improved, and the frictional process once again exhibited the characteristics of boundary friction; thus, the instantaneous friction coefficient showed a stable fluctuation trend. However, due to the damaged frictional surface, the mean friction coefficient in this stage was 0.0587, which is bigger than that in the initial stage.

Nanolubricants

Figure 9 shows the friction coefficient curves under different nanolubricants.

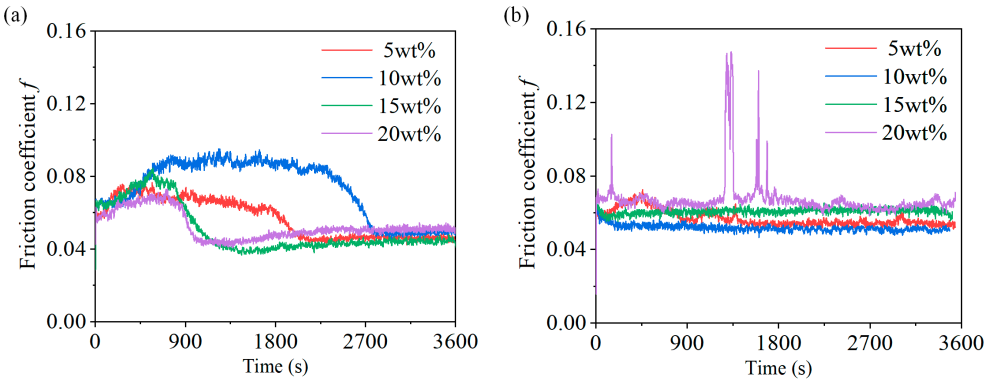


Figure 9. Friction coefficient curves under different nanolubricants: (**a**) MoS_2; (**b**) SiO_2.

(1) Figure 9a indicates that, with the increase in the test time, the friction coefficient under the MoS_2 nanolubricants exhibited a two-stage change trend that is different from that of the base fluid. In the first stage, the friction coefficient increased first and then decreased. In the second stage, a "low amplitude stable fluctuation" feature was observed. In the first stage, the maximum friction coefficients corresponding to the MoS_2 nanolubricants of 5 wt%, 10 wt%, 15 wt%, and 20 wt% were 0.077, 0.095, 0.085, and 0.073, respectively, which are all less than that of the base fluid (f = 0.178). According to the duration and maximum friction coefficient of the first stage, the 20 wt% MoS_2 nanolubricants have the best anti-friction effect, which should be related to their excellent wettability.
(2) Figure 9b shows that the friction coefficient under the SiO_2 nanolubricants was stable as the test time increased and did not show obvious stage characteristics. The maximum friction coefficients were also smaller than that of the base fluid (f = 0.178), and these of the 10 wt% and 15 wt% SiO_2 nanolubricants were all less than 0.06. According to the maximum and fluctuation of the instantaneous friction coefficient, when the additive percentage was 5 wt%, 10 wt%, and 15 wt%, the SiO_2 nanolubricants could achieve a good anti-friction effect, and the effect of the 10 wt% nanolubricant was

the best. However, when the SiO_2 percentage was 20 wt%, the instantaneous friction coefficient increased sharply within a short time. This phenomenon was caused by the increase in the shear resistance due to the excessive additive percentage [41].

In summary, both MoS_2 and SiO_2 nanolubricants exhibit an excellent anti-friction performance. However, the friction coefficients of the two nanolubricants present different variation characteristics with the test time. This result shows that the soft MoS_2 nano-additive and the hard SiO_2 nano-additive have different anti-friction mechanisms at the friction interface.

3.2.2. Abrasion Surface Topography of the Lower Specimen

Figure 10 shows the abrasion surface of the Inconel 718 specimen under the lubrication of the base fluid; severe defects appeared on the abrasion surface, including plastic deformation, microcracks, surface exfoliation, and chipping pits. As shown in Figure 10a, plastic deformation appeared at the edge of the abrasion trace and was caused by the friction and extrusion of the upper specimen. As shown in Figure 10c, microcracks, surface exfoliation, and chipping pits mainly occurred in the middle of the abrasion trace, and the closer they were to the center of the abrasion trace, the more severe the damage was. Microcracks appeared in the middle stage of the friction test because of the collapse of the lubricating film and the fatigue failure of the abrasion surface. In contrast, surface exfoliation and chipping pits were formed by the propagation of microcracks and adhesive wear.

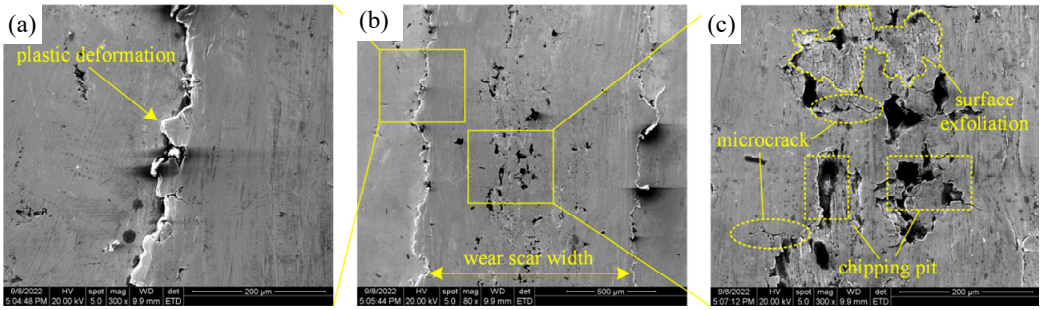


Figure 10. Abrasion surface of the lower specimen under the lubrication of the base fluid: (**a**) edge of the abrasion trace; (**b**) overall view of the abrasion trace; (**c**) middle of the abrasion trace.

Figures 11 and 12 show the abrasion surfaces of the lower specimen under the MoS_2 and SiO_2 nanolubricants, respectively. Compared with Figure 10, the defect form of the abrasion surfaces changed. Although plastic deformation and chipping pits remained, the topographies of the abrasion surfaces, in most cases, significantly improved.

With MoS_2 nanolubricants, furrow and material smearing were the two main topographic characteristics of the abrasion surfaces. Furrow was caused by abrasive wear, which can deteriorate the surface quality. Meanwhile, material smearing was caused by the reciprocating friction and the extrusion of the upper specimen, which can reduce the size of the furrows and improve the surface quality. According to Figure 11a, when the MoS_2 percentage was 5 wt%, chipping pits, furrow, and material smearing simultaneously appeared on the abrasion surface, so the abrasion topography was relatively poor. In this situation, the friction coefficient is large. According to Figure 11b, when the MoS_2 percentage was 10 wt%, the effect of material smearing was weak, but deep furrows appeared on the abrasion surface, so the corresponding friction coefficient fluctuated with a high amplitude for a long time. When the MoS_2 percentage increased from 10 wt% to 20 wt%, the size of the furrows gradually decreased due to the enhancement of the material smearing effect, thereby improving the topography of the abrasion surface and decreasing the duration of the high-amplitude friction coefficient.

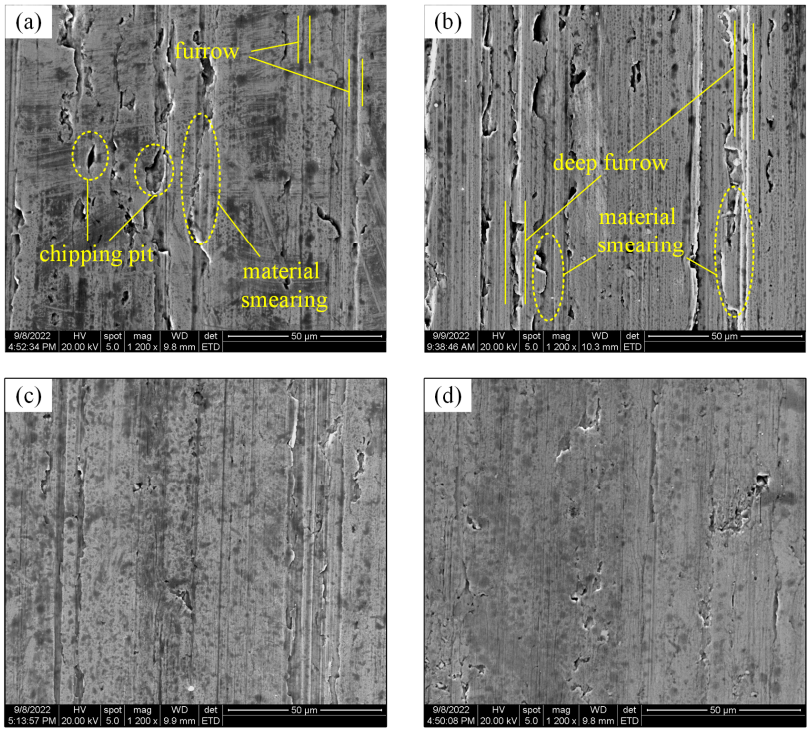


Figure 11. Abrasion surfaces of the Inconel 718 specimen under MoS_2 nanolubricants: (**a**) 5 wt%; (**b**) 10 wt%; (**c**) 15 wt%; (**d**) 20 wt%.

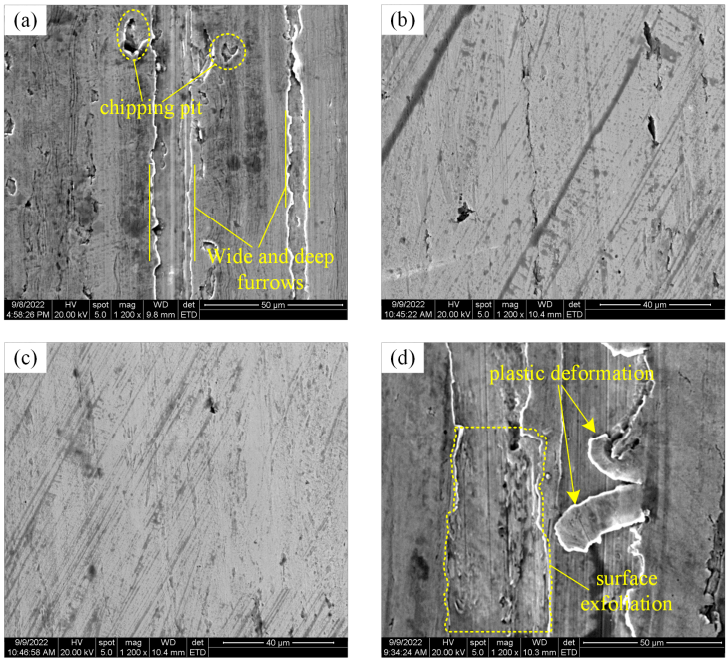


Figure 12. Abrasion surfaces of the lower specimen under SiO_2 nanolubricants: (**a**) 5 wt%; (**b**) 10 wt%; (**c**) 15 wt%; (**d**) 20 wt%.

Compared with the MoS_2 nanolubricants, the SiO_2 nanolubricants have different topographic characteristics of abrasion surfaces. Figure 12a shows that when the SiO_2 percentage was 5 wt%, the abrasion surface had deep furrows and large chipping pits. Accordingly, the friction coefficient was relatively large at the beginning of the test. According to Figure 12b,c, when the SiO_2 percentage was 10 wt% and 15 wt%, the abrasion surfaces were generally smooth in addition to the inclined scratches formed by the rolling of SiO_2 particles. In both cases, the friction coefficient was very stable during the entire

test. Figure 12d shows that when the SiO_2 percentage was 20 wt%, the topography of the abrasion surface was very poor, with serious plastic deformation and surface exfoliation, and the corresponding friction coefficient also fluctuated sharply within a short time, which might be caused by the accumulation and agglomeration of excessive nanoparticles.

The above analysis indicates that the abrasion surfaces of the MoS_2 and SiO_2 nanolubricants have different topography characteristics. Moreover, a close internal relationship exists between the abrasion surface and the friction coefficient, and a smooth and steady friction coefficient represents a good abrasion surface quality.

3.2.3. Abrasion Trace Size of the Lower Specimen

In addition to the topography characteristics of the abrasion surface, the abrasion trace size is also an important index for evaluating the anti-friction performance of lubricants. Figure 13 shows the morphologies of abrasion traces under different lubricants, which were measured using a Contour GT-K 3D surface profiler. As shown in Figure 14, the width and depth of the abrasion traces were obtained from the morphology. In order to eliminate the measurement error caused by uneven plastic deformation at the edge of the abrasion trace, the influence of plastic deformation on the abrasion trace size has been eliminated. According to Figures 13 and 14, the following results can be found.

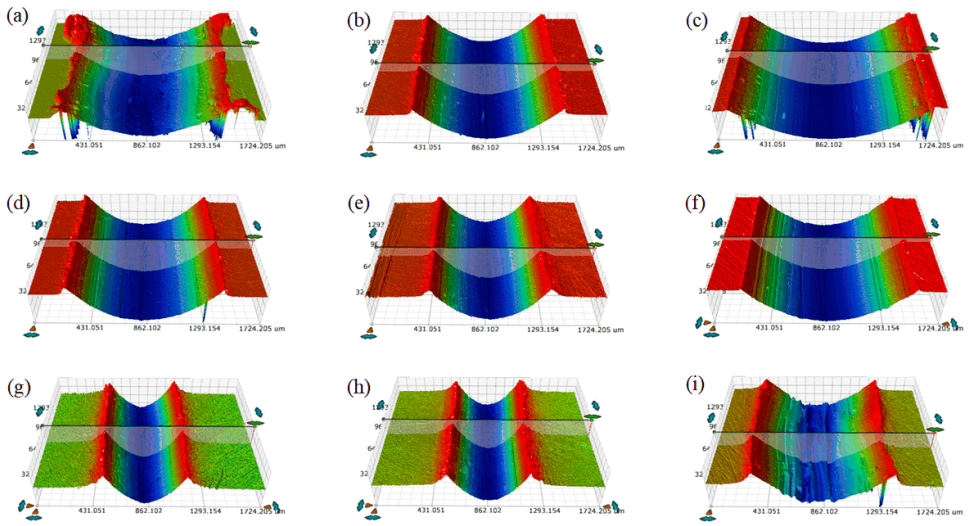


Figure 13. Morphologies of abrasion traces under different lubricants: (**a**) base fluid; (**b**) 5 wt% MoS_2; (**c**) 10 wt% MoS_2; (**d**) 15 wt% MoS_2; (**e**) 20 wt% MoS_2; (**f**) 5 wt% SiO_2; (**g**) 10 wt% SiO_2; (**h**) 15 wt% SiO_2; (**i**) 20 wt% SiO_2.

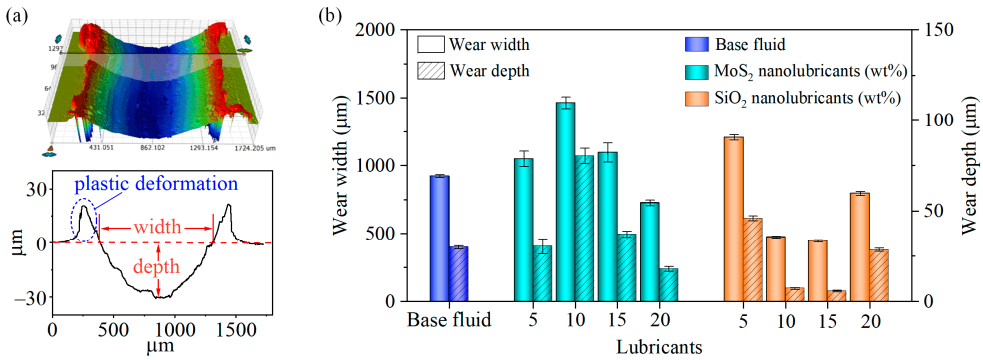


Figure 14. Measurement method and result of abrasion trace size: (**a**) measurement method; (**b**) abrasion trace size.

(1) For MoS_2 nanolubricants, the abrasion trace size was smaller than that of the base fluid only when the additive percentage was 20 wt%. For the SiO_2 nanolubricants, except for the abrasion trace at 5 wt% additive percentage, the size of the other abrasion traces was smaller than that of the base fluid. The abrasion trace size under the 15 wt% SiO_2 nanolubricant was the lowest, with a width and a depth of 51.16% and 80.79% of the base fluid, respectively.

(2) In general, a close relationship exists between the size and surface quality of the abrasion trace. A good surface quality means a small abrasion trace size. For experimental friction pairs, the SiO_2 nanolubricant displayed a better anti-wear effect than the MoS_2 nanolubricants. Whether the tribological performance is evaluated in terms of friction coefficient, abrasion surface quality, or abrasion trace size, the best results were obtained under the 10 wt% and 15 wt% of SiO_2 nanolubricants.

4. Analysis of Action Mechanism for Different Nano-Additives

As shown in Figure 15, during nanofluid lubrication, the action mechanism of nano-additives at the friction interface can be described by four types of effects, namely, the adsorption film, mending, polishing, and rolling effects [42,43].

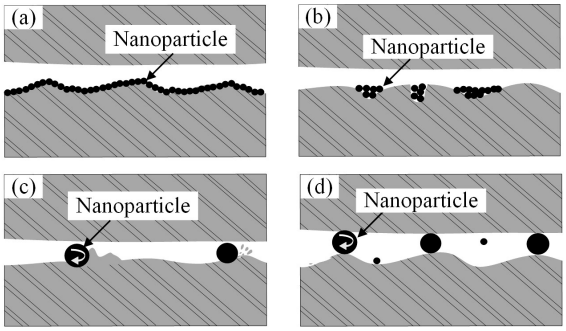


Figure 15. Action mechanism of nano-additives: (**a**) adsorption film effect; (**b**) mending effect; (**c**) polishing effect; (**d**) rolling effect.

Figure 16 shows the element content on the original surface and abrasion surfaces of the Inconel 718 specimen, which is measured by a XFlash Detector 630M energy dispersive spectrometer (Bruker, Billerica, MA, USA). During the measurement, the accelerating voltage was 20 kV, and the magnification was 300. On the basis of the Mo and Si contents, the action mechanism of the MoS_2 and SiO_2 nano-additives can be further analyzed.

(1) According to Figure 16a,b, the Mo and Si contents on the original surface were 3.70% and 0.31%, while the contents on the abrasion surface under the base fluid were 3.53% and 0.52%, respectively. The difference between the two is very small.

(2) Figure 16c,d show that, under the 5 wt% MoS_2 nanolubricant, the Mo contents in the smooth area and severe wear area of the abrasion trace were 8.84% and 12.85%, respectively, which are much higher than the 3.53% under the base fluid, indicating increases of 5.31% and 9.32%, respectively. The significant increase in the Mo content in different areas means that a layer of MoS_2 adsorption film formed on the abrasion surface. Meanwhile, the Mo content in the severe wear area is higher than that in the smooth area, indicating that a great amount of MoS_2 additives was squeezed into the furrows or chipping pits on the abrasion surface, resulting in the mending effect.

(3) According to Figure 16e,f, under the 5 wt% SiO_2 nanolubricants, the Si contents in the smooth area and severe wear area of the abrasion trace were 0.90% and 3.03%, respectively, which are larger than 0.52% under the base fluid, indicating increases of only 0.38% and 2.51%, respectively. This result indicates that the adsorption film and

mending effects of SiO_2 additives are not obvious. Therefore, the improvement of the anti-friction performance of SiO_2 nanolubricants should be mainly attributed to the rolling and polishing effects of hard SiO_2 additives, which transform sliding friction into rolling friction between the friction pairs.

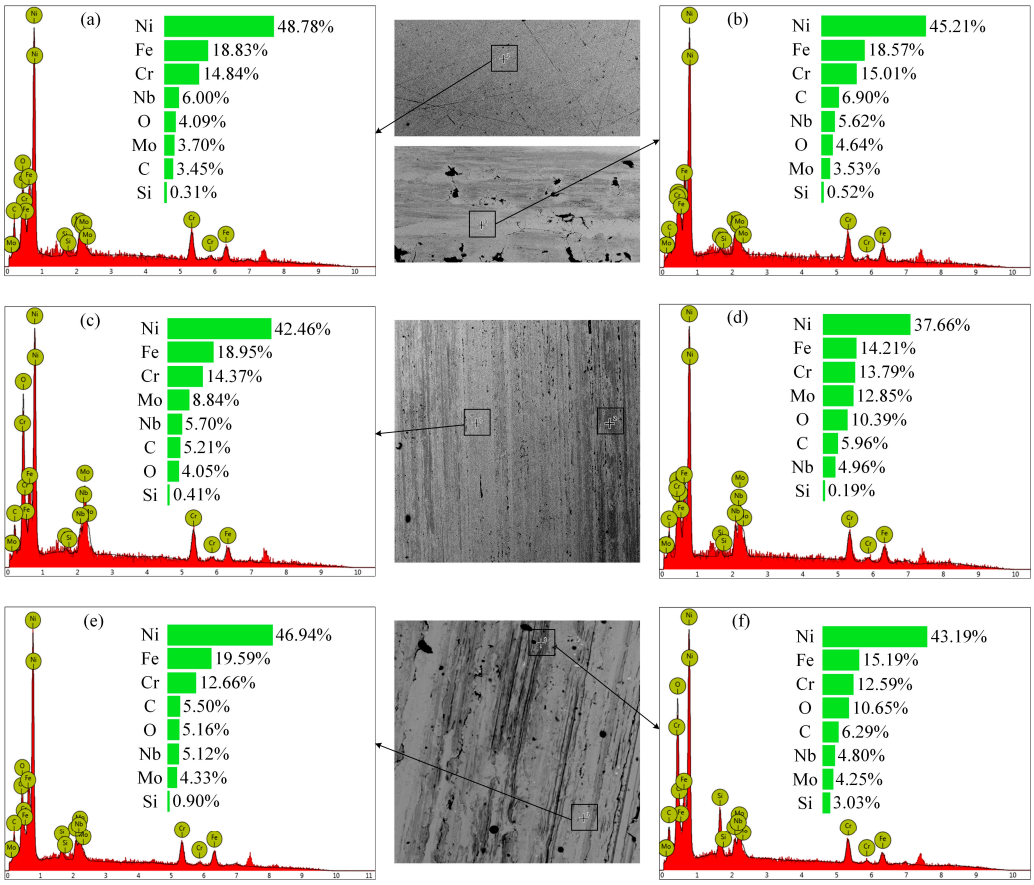


Figure 16. Element content on the original surface and abrasion surfaces of the Inconel 718 specimen: (**a**) original surface; (**b**) abrasion surface under the base fluid; (**c**) smooth area of abrasion surface under 5 wt% MoS_2 nanolubricant; (**d**) severe wear area of abrasion surface under 5 wt% MoS_2 nanolubricant; (**e**) smooth area of abrasion surface under 5 wt% SiO_2 nanolubricant; (**f**) severe wear area of abrasion surface under 5 wt% SiO_2 nanolubricant.

5. Conclusions

(1) MoS_2 and SiO_2 nano-additives could improve the viscosity of mineral oil and change its wettability. And there was a certain correlation between the viscosity and wettability of nanolubricants. Due to the differences in physical properties of the two additives, the wettability of MoS_2 and SiO_2 nanolubricants exhibited different variation trends with their viscosity. The wettability of the MoS_2 nanolubricants increased with the viscosity, while the wettability of the SiO_2 nanolubricants decreased.

(2) Although MoS_2 and SiO_2 nanolubricants had different change characteristics of friction coefficient with the frictional time, their maximum and fluctuation values were all smaller than those of base liquid. For MoS_2 nanolubricant, when the additive percentage was 20 wt%, the friction coefficient curve fluctuated the least, and the maximum value was 0.073, which was much smaller than 0.178 of the base fluid. For the SiO_2 nanolubricant, the best anti-friction effect was achieved when the additive percentage was 10 wt%, and the maximum friction coefficient was less than 0.06.

(3) Compared with the base fluid, the nanolubricants can improve the surface quality of abrasion traces. However, the abrasion surfaces of the two nanolubricants had

different topography characteristics. Furrow and material smearing were the two main topography features under the MoS_2 nanolubricant. And, with the rise in MoS_2 percentage, the effect of material smearing was enhanced, and the surface quality of the abrasion trace was improved. With the change in SiO_2 percentage, the abrasion surface quality showed a trend of first improvement and then deterioration, and the surface quality with 10 wt% and 15 wt% SiO_2 nanolubricant was better.

(4) A close internal relationship exists between friction coefficient, abrasion surface quality, and abrasion trace size. A steady friction coefficient represents a good abrasion surface quality and a small abrasion trace size. For the experimental friction pairs, the SiO_2 nanolubricant has a better anti-friction effect than MoS_2 nanolubricants. With 10 wt% and 15 wt% SiO_2 nanolubricants, the width and depth of abrasion traces were about half those of the base fluid.

(5) The soft MoS_2 nano-additive and the hard SiO_2 nano-additive have different anti-friction mechanisms. The action mechanism of the MoS_2 nano-additive is the adsorption film effect and mending effect of nanoparticles, while the main action mechanism of the SiO_2 nano-additive should be the polishing effect and rolling effect of nanoparticles.

Author Contributions: Methodology, L.M. and Q.F.; experiments and data analysis, F.L. and Z.M.; software, S.B. and X.M.; writing—original draft preparation, Z.M. and F.L.; writing—review and editing, L.M. and K.Y. All authors have read and agreed to the published version of the manuscript.

Funding: This research was financially supported by the National Natural Science Foundation of China, Grant Number 52175397.

Data Availability Statement: All data generated or analyzed during this study are included in this article.

Conflicts of Interest: The authors declare no conflicts of interest.

References

1. Holmberg, K.; Erdemir, A. Influence of tribology on global energy consumption, costs and emissions. *Friction* **2017**, *5*, 263–284. [CrossRef]
2. Brinksmeier, E.; Meyer, D.; Huesmann-Cordes, A.G.; Herrmann, C. Metalworking fluids—Mechanisms and performance. *CIRP Annals.* **2015**, *64*, 605–628. [CrossRef]
3. Öndin, O.; Kıvak, T.; Sarıkaya, M.; Yıldırım, Ç.V. Investigation of the influence of MWCNTs mixed nanofluid on the machinability characteristics of PH 13-8 Mo stainless steel. *Tribol. Int.* **2020**, *148*, 106323. [CrossRef]
4. Shariatmadar, F.S.; Pakdehi, S.G. Synthesis and characterization of aviation turbine kerosene nanofluid fuel containing boron nanoparticles. *Energy Fuels.* **2016**, *30*, 7755–7762. [CrossRef]
5. Wang, X.; Li, C.; Zhang, Y.; Ali, H.M.; Sharma, S.; Li, R.; Yang, M.; Said, Z.; Liu, X. Tribology of enhanced turning using biolubricants: A comparative assessment. *Tribol. Int.* **2022**, *174*, 107766. [CrossRef]
6. Saidur, R.; Kazi, S.N.; Hossain, M.S.; Rahman, M.M.; Mohammed, H.A. A review on the performance of nanoparticles suspended with refrigerants and lubricating oils in refrigeration systems. *Renew. Sustain. Energy Rev.* **2011**, *15*, 310–323. [CrossRef]
7. Kotia, A.; Rajkhowa, P.; Rao, G.S.; Ghosh, S.K. Thermophysical and tribological properties of nanolubricants: A review. *Heat Mass Transf.* **2018**, *54*, 3493–3508. [CrossRef]
8. Dai, W.; Kheireddin, B.; Gao, H.; Liang, H. Roles of nanoparticles in oil lubrication. *Tribol. Int.* **2016**, *102*, 88–98. [CrossRef]
9. Wang, B.; Qiu, F.; Barber, G.C.; Zou, Q.; Wang, J.; Guo, S.; Yuan, Y.; Jiang, Q. Role of nano-sized materials as lubricant additives in friction and wear reduction: A review. *Wear* **2022**, *490*, 204206. [CrossRef]
10. Jatti, V.S.; Singh, T.P. Copper oxide nano-particles as friction-reduction and anti-wear additives in lubricating oil. *J. Mech. Sci. Technol.* **2015**, *29*, 793–798. [CrossRef]
11. Sia, S.Y.; Sarhan, A.A.D. Morphology investigation of worn bearing surfaces using SiO_2 nanolubrication system. *Int. J. Adv. Manuf. Technol.* **2014**, *70*, 1063–1071. [CrossRef]
12. Sujan, K.; Wang, B.; Hu, M.; Meng, S.; Zhang, L.; Hu, R.; Barber, G.C. Tribological properties of Al_2O_3/WS_2 oil-based composite lubricant utilized on steel-brass frictional couples. *Surf. Topogr. Metrol. Prop.* **2021**, *9*, 015018. [CrossRef]

13. Su, Y.; Gong, L.; Chen, D. An investigation on tribological properties and lubrication mechanism of graphite nanoparticles as vegetable based oil additive. *J. Nanomater.* **2015**, *2015*, 276753. [CrossRef]
14. Yu, R.; Liu, J.; Zhou, Y. Experimental study on tribological property of MoS_2 nanoparticle in castor oil. *J. Tribol.* **2019**, *141*, 102001. [CrossRef]
15. Mo, Y.H.; Tao, D.H.; Wei, X.C. Activation and self-repairing effectiveness of lubrication with nano-tin as additives. *J. Shanghai Univ. Engl. Ed.* **2009**, *13*, 45–50. [CrossRef]
16. Singh, Y.; Singh, N.K.; Sharma, A. Effect of SiO_2 nanoparticles on the tribological behavior of Balanites Aegytiaca (Desert date) oil-based biolubricant. *J. Bio Tribo-corros.* **2021**, *7*, 1–6. [CrossRef]
17. Chu, H.Y.; Hsu, W.C.; Lin, J.F. The anti-scuffing performance of diamond nano-particles as an oil additive. *Wear* **2010**, *268*, 960–967. [CrossRef]
18. Gupta, M.K.; Bijwe, J. A complex interdependence of dispersant in nano-suspensions with varying amount of graphite particles on its stability and tribological performance. *Tribol. Int.* **2020**, *142*, 105968. [CrossRef]
19. Luo, T.; Wei, X.; Huang, X.; Huang, L.; Yang, F. Tribological properties of Al_2O_3 nanoparticles as lubricating oil additives. *Ceram. Int.* **2014**, *40*, 7143–7149. [CrossRef]
20. Peyghambarzadeh, S.M.; Hashemabadi, S.H.; Jamnani, M.S.; Hoseini, S.M. Improving the cooling performance of automobile radiator with Al_2O_3/water nanofluid. *App. Therm. Eng.* **2011**, *31*, 1833–1838. [CrossRef]
21. Mohamed, K.A.A.; Hou, X.J.; Abdelkareem, M.A.A. Anti-wear properties evaluation of frictional sliding interfaces in automobile engines lubricated by copper/graphene nanolubricants. *Friction* **2020**, *8*, 905–916.
22. Kulkarni, D.P.; Vajjha, R.S.; Das, D.K.; Oliva, D. Application of aluminum oxide nanofluids in diesel electric generator as jacket water coolant. *App. Therm. Eng.* **2008**, *28*, 1774–1781. [CrossRef]
23. Buongiorno, J.; Hu, L.W.; Kim, S.J.; Hannink, R.; Truong, B.A.O.; Forrest, E. Nanofluids for enhanced economics and safety of nuclear reactors: An evaluation of the potential features, issues, and research gaps. *Nucl. Technol.* **2008**, *162*, 80–91. [CrossRef]
24. Syafiq, A.M.; Redhwan, A.A.M.; Hazim, A.A.; Aminullah, A.R.M.; Ariffin, S.Z.; Nughoro, W.; Arifuddin, A.; Hawa, A.B.S. An Experimental Evaluation of SiO_2 nano cutting fluids in CNC Turning of Aluminium Alloy AL319 via MQL Technique. *IOP Conf. Ser. Mater. Sci. Eng.* **2021**, *1068*, 012009. [CrossRef]
25. Ni, J.; Cui, Z.; He, L.; Yang, Y.; Sang, Z.; Rahman, M.M. Reinforced lubrication of vegetable oils with nano-particle additives in broaching. *J. Manuf. Process.* **2021**, *70*, 518–528. [CrossRef]
26. Pal, A.; Chatha, S.S.; Sidhu, H.S. Performance evaluation of the minimum quantity lubrication with Al_2O_3-mixed vegetable-oil-based cutting fluid in drilling of AISI 321 stainless steel. *J. Manuf. Process.* **2021**, *66*, 238–249. [CrossRef]
27. Gajrani, K.K.; Ram, D.; Sankar, M.R. Biodegradation and hard machining performance comparison of eco-friendly cutting fluid and mineral oil using flood cooling and minimum quantity cutting fluid techniques. *J. Clean. Prod.* **2017**, *165*, 1420–1435. [CrossRef]
28. Okokpujie, I.P.; Tartibu, L.K. Experimental analysis of cutting force during machining difficult to cut materials under dry, mineral oil, and TiO_2 nano-lubricant. *J. Meas. Eng.* **2021**, *9*, 218–230. [CrossRef]
29. Harsha, A.P.; Khatri, O.P. The Effect of Spherical Hybrid Silica-Molybdenum Disulfide on the Lubricating Characteristics of Castor Oil. *J. Tribol.* **2023**, *145*, 121701-1.
30. Prasad, B.K.; Rathod, S.; Yadav, M.S.; Modi, O.P. Effects of some solid lubricants suspended in oil toward controlling the wear performance of a cast iron. *J. Tribol.* **2010**, *132*, 041602. [CrossRef]
31. Yegin, C.; Lu, W.; Kheireddin, B.; Zhang, M.; Li, P.; Min, Y.; Sue, H.J.; Sari, M.M.; Akbulut, M. The effect of nanoparticle functionalization on lubrication performance of nanofluids dispersing silica nanoparticles in an ionic liquid. *J. Tribol.* **2017**, *139*, 041802. [CrossRef]
32. Basso, C.R.; Crulhas, B.P.; Castro, G.R.; Pedrosa, V.A. A study of the effects of pH and surfactant addition on gold nanoparticle aggregation. *J. Nanosci. Nanotechnol.* **2020**, *20*, 5458–5468. [CrossRef] [PubMed]
33. Bao, L.; Zhong, C.; Jie, P.; Hou, Y. The effect of nanoparticle size and nanoparticle aggregation on the flow characteristics of nanofluids by molecular dynamics simulation. *Adv. Mech. Eng.* **2019**, *11*, 1–17. [CrossRef]
34. Xu, M.H.; Cao, Y.Y.; Gao, S.G. Surface modification of nano-silica with silane coupling agent. *Key Eng. Mater.* **2015**, *636*, 23–27. [CrossRef]
35. Hou, X.; Jiang, H.; Ali, M.K.A.; Liu, H.; Su, D.; Tian, Z. Dispersion behavior assessment of the molybdenum disulfide nanomaterials dispersed into poly alphaolefin. *J. Mol. Liq.* **2020**, *311*, 113303. [CrossRef]
36. Harigaya, Y.; Suzuki, M.; Toda, F.; Takiguchi, M. Analysis of oil film thickness and heat transfer on a piston ring of a diesel engine: Effect of lubricant viscosity. *J. Eng. Gas Turbines Power* **2006**, *128*, 685–693. [CrossRef]
37. Singh, J.; Kumar, D.; Tandon, N. Development of nanocomposite grease: Microstructure, flow, and tribological studies. *J. Tribol.* **2017**, *139*, 052001.
38. Parizad, A.; Shahbazi, K.; Tanha, A.A. SiO_2 nanoparticle and KCl salt effects on filtration and thixotropical behavior of polymeric waterbased drilling fluid: With zeta potential and size analysis. *Results Phys.* **2018**, *9*, 1656–1665. [CrossRef]

39. Sanukrishna, S.S.; Vishnu, S.; Prakash, M.J. Experimental investigation on thermal and rheological behaviour of PAG lubricant modified with SiO_2 nanoparticles. *J. Mol. Liq.* **2018**, *261*, 411–422. [CrossRef]
40. Basha, M.M.; Sankar, M.R. Experimental tribological study on additive manufactured Inconel 718 features against the hard carbide counter bodies. *J. Tribol.* **2023**, *145*, 121702.
41. Sajeeb, A.; Krishnan Rajendrakumar, P. Experimental studies on viscosity and tribological characteristics of blends of vegetable oils with CuO nanoparticles as additive. *Micro Nano Lett.* **2019**, *14*, 1121–1125. [CrossRef]
42. Jason, Y.J.J.; How, H.G.; Teoh, Y.H.; Chuah, H.G. A study on the tribological performance of nanolubricants. *Processes* **2020**, *8*, 1372. [CrossRef]
43. Cui, X.; Li, C.; Ding, W.F.; Chen, Y.; Mao, C.; Xu, X.F.; Liu, B.; Wang, D.Z.; Li, H.N.; Zhang, Y.B.; et al. Minimum quantity lubrication machining of aeronautical materials using carbon group nanolubricant: From mechanisms to application. *Chin. J. Aeronaut.* **2022**, *35*, 85–112. [CrossRef]

Disclaimer/Publisher's Note: The statements, opinions and data contained in all publications are solely those of the individual author(s) and contributor(s) and not of MDPI and/or the editor(s). MDPI and/or the editor(s) disclaim responsibility for any injury to people or property resulting from any ideas, methods, instructions or products referred to in the content.